A mathematical model of the *Drosophila* circadian clock with emphasis on posttranslational mechanisms

Tanya L. Leise *, Emily E. Moin [1]

Mathematics and Computer Science Department, Amherst College, Amherst, MA 01002 USA

Abstract

Experimental evidence points increasingly to the importance of posttranslational processes such as phosphorylation and translocation in the molecular circadian clocks of many organisms. We develop a mathematical model of the *Drosophila* circadian clock that incorporates the emerging details of the timing of nuclear translocation of the PERIOD and TIMELESS proteins. Most models assume that these proteins enter the nucleus as a complex, but recent experiments suggest that they in fact enter the nucleus separately. Our model reproduces observed patterns of intracellular localization of PERIOD and TIMELESS during light-dark cycles and in constant darkness, as well as phenotypes of several clock mutants. We also use the model to demonstrate how the *Drosophila* clock can exhibit robust oscillations with constant mRNA levels of *period* or *timeless*, and propose a possible mechanism for oscillations in double rescue experiments of per^{01}-tim^{01} mutants. The model also explains (via posttranslational processes) the counter-intuitive observation that total dCLOCK levels are at their lowest at the circadian time when active nuclear dCLOCK must be peaking in order to activate transcription of other clock genes,

implying that for dCLOCK a posttranslationally-generated rhythm is more important than the transcriptionally-generated rhythm. These results support the idea that posttranslational processes play key roles in generating as well as modulating robust circadian oscillations. While it appears that posttranslational mechanisms alone are not sufficient to generate rhythms in *Drosophila*, posttranslational mechanisms can greatly amplify a very weak transcriptional rhythm.

Key words: Circadian rhythms, Clock genes, Posttranslational processes

1 Introduction

As life evolved on our rotating world, many organisms developed endogenous circadian (∼24 h) clocks. These clocks are able to entrain to the 24 hour light-dark (LD) cycle, but also exhibit, in the absence of external cues, robust free-running oscillations with periods near 24 hours. The basis for the endogenous clock lies in the rhythmic expression of certain clock genes together with a variety of posttranslational mechanisms such as phosphorylation and translocation. For a review, see Allada et al. (2001) or Young and Kay (2001).

Models of circadian rhythms typically view transcriptional-translational feedback loops as the drivers of oscillations, with posttranslational processes viewed as a means of adjusting the amplitude and the period length. Multiple transcriptional-translational feedback loops can potentially facilitate multiple input and

* Corresponding author. Email: tleise@amherst.edu; Tel.: (413)542-5411; FAX: (413)542-2550.

[1] The second author gratefully acknowledges the support of a Howard Hughes Medical Institute Summer Fellowship.

output pathways (Cyran et al., 2003), as well as temperature compensation (Ruoff et al., 2005). On the other hand, Lakin-Thomas (2006) has recently suggested that we should consider whether we have overemphasized the role of rhythmic transcription (or perhaps underemphasized the role of other processes), particularly in light of experiments for which purely posttranslational processes generate a robust circadian rhythm, for example, rhythmic *in vitro* phosphorylation and dephosphorylation of the KaiC protein in cyanobacteria (Nakajima et al., 2005). Others, including Kiyohara et al. (2006), have put forth the possibility that posttranslational mechanisms regulated by kinase activity form the core of the circadian clock, while rhythmic transcription adds robustness and amplitude to the oscillations. Other posttranscriptional and posttranslational processes may also play important roles in the clock mechanism; for a review of these processes, see Harms et al. (2004).

The circadian clock of *Drosophila* has been extensively studied as a model system for molecular chronobiology. Briefly, dCLOCK (CLK) and CYCLE (CYC) proteins form a complex which activates transcription of the *period* (*per*) and *timeless* (*tim*) genes. In turn, the PER and TIM proteins associate in the cytoplasm and eventually move to the nucleus, where PER fully and PER-TIM partially inhibit the transcriptional activation of CLK-CYC by forming a complex with it (Rothenfluh et al., 2000). Light results in the degradation of TIM, thereby providing a highly effective means of shifting the phase of the clock, for instance, by releasing PER in the nucleus from the PER-TIM complex, resulting in strong downregulation of *per* and *tim* expression (Rothenfluh et al., 2000). See Price (2004) and references therein for a more detailed discussion of these clock genes.

Rhythmic expression of the clock genes occurs both in various areas of the

brain and in peripheral tissues like antennae, male reproductive tissues, and eyes (Levine, 2004). In the accessory medulla of each fly are typically 16 ventral-lateral neurons (vLNs); some are classified as "small" and others as "large." The pacemaker for locomotor activity appears to be located in the small vLNs, which express the neurotransmitter *pdf*, while the large vLNs receive input from the retina and so may play a key role in light entrainment. Rieger et al. (2006) recently did a functional analysis of the roles of vLNs and hypothesize that a subgroup of the small vLNs acts as the main oscillator controlling morning and evening activity bouts in *Drosophila*. The small and large vLNs exhibit differing profiles of TIM oscillation in general and of nuclear accumulation in particular, suggesting that TIM may have different functions in small and large vLNs (Yang and Sehgal, 2001; Shafer et al., 2002). Such differences may support the different roles of the small and large vLNs, given the importance of TIM in entrainment and phase-shifting. Expression profiles of the clock genes also differ among the autonomous peripheral clocks, which have quite different functions specific to each tissue. Given this variety of *Drosophila* clocks, we focus on the small vLNs as important pacemakers, but we expect that appropriate adjustments of model parameters will likely yield valid models for the various other rhythmic tissues.

Most mathematical models of the *Drosophila* molecular clock focus on transcriptional-translational feedback loop(s) as the generators of rhythmicity, with posttranslational processes acting to adjust period and amplitude. The model of Leloup and Goldbeter (1998) is based on direct negative feedback of a nuclear PER-TIM complex on *per* and *tim* transcription and incorporates multiple phosphorylation of PER and TIM as a delaying mechanism. The model of Ueda et al. (2001) includes expression of the *clk* gene, leading to two interlocked

feedback loops. The model of Smolen et al. (2004) focuses on the additional feedback loops involving *Pdp-1* and *vri* (but neglects *tim*). Ruoff et al. (2005) explore mechanisms of temperature compensation via a model with a *Pdp1*-mediated positive feedback loop as well as the negative feedback loop involving PER-TIM and CLK. All of these models have in common the assumption that PER and TIM proteins enter the nucleus as a complex. These models display robust oscillations and behavior consistent with many experimental results, including reproducing some mutant phenotypes. However, ignoring important posttranslational processes can lead to predictions of arrhythmicity in the absence of rhythmic transcription, contrary to the findings of rhythmic mutants with constant RNA levels of *per* (Frisch et al., 1994; Vosshall and Young, 1995; Cheng and Hardin, 1998) or of *tim* or both *tim* and *per* (Yang and Sehgal, 2001), as pointed out by Lakin-Thomas (2006).

The model presented in this article (see Figure 1) modifies and extends previous models like that of Ueda et al. (2001) to include posttranslational processes regulating the translocation of PER and TIM to the nucleus. Recent experimental results (Shafer et al., 2002; Cyran et al., 2005) suggest that PER and TIM may enter the nucleus separately, as the data show a significant lag between peak times of PER and TIM protein accumulation in the nucleus. The dramatic movies produced by Meyer and Young (2006) directly demonstrate the abillity of PER and TIM proteins to enter the nucleus separately in the S2 *Drosophila* cell line. PER tends to accumulate in the nucleus in the absence of DOUBLETIME (DBT) and TIM (Price et al., 1998; Cyran et al., 2005), while TIM tends to accumulate in the cytoplasm in the absence of PER (Myers et al., 1996), leading to the possibility that these opposing tendencies may turn nuclear entry of these proteins into a switch, as suggested by Cyran et al.

(2005). Such a switch may be controlled in large part by the kinase activity of DBT and SHAGGY (SGG) in the cytoplasm. DBT promotes degradation of PER, which is suppressed when PER associates with TIM (Kloss et al., 2001). The kinase activity of SGG appears to promote nuclear entry of TIM (Martinek et al., 2001). Based on these recent experimental results, Cyran et al. (2005) hypothesize that the function of the PER-TIM complex in the cytoplasm may be to time the translocation from cytoplasm to nucleus of these proteins, with the length of the delay regulated by kinase activity.

Using these findings, we develop a model whose major departure from previous *Drosophila* circadian clock models is the treatment of the PER-TIM complex and its roles in circadian oscillations. In previous models, the association of PER and TIM in the cytoplasm provides the mechanism for nuclear entry. In our model, the main function of this association (which is assumed to happen fairly quickly and not be a source of delay) is to stabilize PER and retain it in the cytoplasm. Experimental results support the proposition that PER and TIM remain dimerized through most of their several hour stay in the cytoplasm before dissociating and entering the nucleus separately, at different times (Shafer et al., 2002; Cyran et al., 2005; Meyer and Young, 2006). The SGG protein promotes phosphorylation of cytoplasmic TIM, and overexpression of SGG results in shortened periods while underexpression results in lengthened periods (Martinek et al., 2001). This suggests that the prolonged accumulation of PER and TIM in the cytoplasm is a result of the lag before TIM has been sufficiently phosphorylated (or modified by some other post-translational process) to dissociate from PER and enter the nucleus.

Another important consideration for the modeling concerns the CLK-CYC complex, part of the positive limb of the main feedback loop. CYC is constitu-

tively highly abundant, but CLK is a limiting quantity in the clock mechanism (Bae et al., 2000). The total amount of CLK protein at its peak (∼ZT 0-4) is several fold lower than that of PER or TIM at their peak (∼ZT16-20) (Bae et al., 2000). It also appears that CLK protein levels can peak slightly before *clk* mRNA levels and that the mRNA and protein oscillations are closely in phase (Lee et al., 1998), as opposed to the cases of *per* and *tim* for which

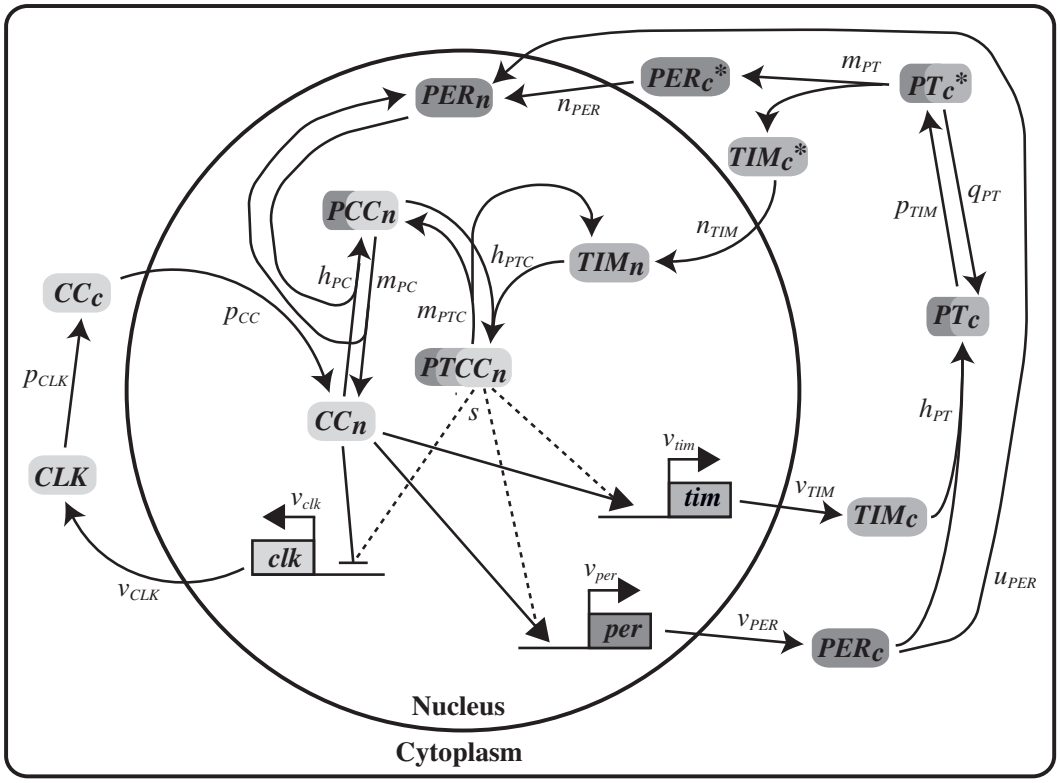

Fig. 1. The model of the *Drosophila* molecular clock mechanism within a small vLN. In the cytoplasm, CLK protein associates with CYC (CC_c) and then enters the nucleus. Transcription of the clock genes *per* and *tim* is activated by nuclear CLK-CYC (CC_n), which inhibits transcription of *clk*. The PER (PER_c) and TIM (TIM_c) proteins form a heterodimer (PT_c) in the cytoplasm, which undergoes modifications (PT_c^*) and eventually disassociates into PER_c^* and TIM_c^*. These modified proteins may then enter the nucleus (PER_n and TIM_n) and associate with CC_n (to become PCC_n or $PTCC_n$).

the protein peak lags the mRNA peak by roughly 6 hours. (It is interesting that a similar behavior appears in *Bmal1* oscillations in the mouse liver (Lee et al., 2001)). The mechanism of this unexpected behavior may be due to differences in degradation mechanisms between CLK and PER proteins, or to some unaccounted-for posttranscriptional regulation of *clk* RNA. The fact that these data are from head extracts may be important, given the essential differences in the PER and TIM rhythms between large and small vLNs observed by Shafer et al. (2002), and the fact that CLK is also found in non-oscillating cells (Houl et al., 2006).

An intriguing feature of CLK oscillation is the trough of overall abundance around ZT12, precisely the time when the active nuclear CLK must be peaking in order to activate transcription of clock genes. These properties of CLK rhythm have not been reproduced by previous models like that of Ueda et al. (2001), and they highlight the importance of posttranslational mechanisms in producing oscillations. Our model demonstrates that through posttranslational mechanisms, the abundance of active CLK-CYC can indeed peak during the same time that the total CLK abundance is at its lowest value.

There is another possibility to explain the odd timing of CLK oscillations. It could be that the CLK oscillation is an artifact of a particular measurement technique. Houl et al. (2006) recently observed, using a new CLK antibody, that CLK accumulates primarily in the nucleus and appears to remain at fairly constant levels, in contrast to Western blot results. We also consider this possibility via a reduced model that assumes constant nuclear CLK abundance.

2 Mathematical modeling

The model, given in Figure 2, consists of 16 differential equations modeling the interlocked *per*, *tim* and *clk* loops, with special consideration given to the post-translational behavior of PER and TIM. These equations are derived in part from the model of 10 differential equations proposed by Ueda et al. (2001), although with significant modifications and additions, including a major change in the role of the PER-TIM complex. We also include the binding of PER and PER-TIM to CLK-CYC in the nucleus to fully or partially inhibit transcriptional activation, handled in a similar manner as the analogous mechanism in the mammalian model of Leloup and Goldbeter (2004).

The model given in Figure 2 is based on the following assumptions:

(1) CYC, DBT, and SGG are constitutively abundant.

(2) CLK protein can activate transcription of *per* and *tim* after associating with CYC, undergoing posttranslational modifications such as phosphorylation, and entering the nucleus. These posttranslational modifications are represented by the sequence CLK_c (hypophosphorylated CLK protein in the cytoplasm), CC_c (phosphorylated CLK in the cytoplasm which is in a complex with CYC), and CC_n (fully phosphorylated CLK-CYC in the nucleus).

(3) We neglect the further feedback loops involving *Pdp-1* and *vri*, and assume a negative feedback on *clk* by active nuclear CYC-CLK complexes, as is done in the model of Ueda et al. (2001).

(4) PER fully inhibits the transcriptional activity of CLK-CYC in the nucleus by forming a complex with it (PCC_n), while PER-TIM is only partially

inhibiting ($PTCC_n$). Hence the mRNA synthesis terms involve $CC_n + sPTCC_n$, where s is a constant between 0 and 1 that represents the partial transcriptional activity of PER-TIM-CLK-CYC. Note that the

$$
\begin{aligned}
\frac{dClk_m}{dt} &= \frac{v_{clk}k_1^2}{k_1^2 + (CC_n + sPTCC_n)^2} - \frac{d_1 Clk_m}{g_1 + Clk_m} - d_N Clk_m,\\
\frac{dCLK}{dt} &= v_{CLK} Clk_m - \frac{p_{CLK}CLK}{k_2 + CLK} - \frac{d_2 CLK}{g_2 + CLK} - d_{CLK} CLK,\\
\frac{dCC_c}{dt} &= \frac{p_{CLK}CLK}{k_2 + CLK} - \frac{p_{CC}CC_c}{k_3 + CC_c} - \frac{d_3 CC_c}{g_3 + CC_c} - d_{CC} CC_c,\\
\frac{dCC_n}{dt} &= \frac{p_{CC}CC_c}{k_3 + CC_c} - h_{PC} CC_n PER_n + m_{PC} PCC_n - \frac{d_4 CC_n}{g_4 + CC_n} - d_N CC_n,\\
\frac{dPer_m}{dt} &= \frac{v_{per}(CC_n + sPTCC_n)^2}{k_5^2 + (CC_n + sPTCC_n)^2} - \frac{d_5 Per_m}{g_5 + Per_m} - d_N Per_m,\\
\frac{dTim_m}{dt} &= \frac{v_{tim}(CC_n + sPTCC_n)^2}{k_6^2 + (CC_n + sPTCC_n)^2} - \frac{d_6 Tim_m}{g_6 + Tim_m} - d_N Tim_m,\\
\frac{dPER_c}{dt} &= v_{PER} Per_m - h_{PT} PER_c TIM_c - u_{PER} PER_c + d_L PT_c - \frac{d_7 PER_c}{g_7 + PER_c} - d_{PER} PER_c,\\
\frac{dTIM_c}{dt} &= v_{TIM} Tim_m - h_{PT} PER_c TIM_c - d_L TIM_c - \frac{d_8 TIM_c}{g_8 + TIM_c} - d_{TIM} TIM_c,\\
\frac{dPT_c}{dt} &= h_{PT} PER_c TIM_c - \frac{p_{TIM} PT_c}{k_9 + PT_c} + \frac{q_{PT} PT_c^*}{k_{10} + PT_c^*} - d_L PT_c - \frac{d_9 PT_c}{g_9 + PT_c} - d_N PT_c,\\
\frac{dPT_c^*}{dt} &= \frac{p_{TIM} PT_c}{k_9 + PT_c} - \frac{q_{PT} PT_c^*}{k_{10} + PT_c^*} - m_{PT} PT_c^* - d_L PT_c^* - \frac{d_{10} PT_c^*}{g_{10} + PT_c^*} - d_N PT_c^*,\\
\frac{dPER_c^*}{dt} &= m_{PT} PT_c^* - n_{PER} PER_c^* + d_L PT_c^* - \frac{d_{11} PER_c^*}{g_{11} + PER_c^*} - d_N PER_c^*,\\
\frac{dTIM_c^*}{dt} &= m_{PT} PT_c^* - n_{TIM} TIM_c^* - d_L TIM_c^* - \frac{d_{12} TIM_c^*}{g_{12} + TIM_c^*} - d_N TIM_c^*,\\
\frac{dPER_n}{dt} &= u_{PER} PER_c + n_{PER} PER_c^* + m_{PC} PCC_n - h_{PC} CC_n PER_n - \frac{d_{13} PER_n}{g_{13} + PER_n} - d_N PER_n,\\
\frac{dTIM_n}{dt} &= n_{TIM} TIM_c^* - d_L TIM_n - h_{PTC} TIM_n PCC_n + m_{PTC} PTCC_n - \frac{d_{14} TIM_n}{g_{14} + TIM_n} - d_N TIM_n,\\
\frac{dPCC_n}{dt} &= h_{PC} CC_n PER_n - m_{PC} PCC_n - h_{PTC} TIM_n PCC_n + m_{PTC} PTCC_n + d_L PTCC_n - \frac{d_{15} PCC_n}{g_{15} + PCC_n} - d_N PCC_n,\\
\frac{dPTCC_n}{dt} &= h_{PTC} TIM_n PCC_n - m_{PTC} PTCC_n - d_L PTCC_n - \frac{d_{16} PTCC_n}{g_{16} + PTCC_n} - d_N PTCC_n.
\end{aligned}
$$

Fig. 2. Differential equations describing the molecular clock mechanism of *Drosophila*. Clk_m, Per_m, and Tim_m represent the abundance of *clk*, *per*, and *tim* mRNA, respectively. To describe transcription, we use Hill equations with Hill coefficient equal to 2, while the translation rates are assumed proportional to the mRNA abundance. Degradation is described by a Michaelis-Menten-type term plus a linear term. The subscript c indicates abundance of a protein in the cytoplasm, while n indicates nuclear protein. The superscript $*$ indicates a posttranslationally modified quantity, e.g., multiply phosphorylated. PT represents the abundance of PER-TIM heterodimers, while CC represents the CLK-CYC heterodimer, PCC the PER-CLK-CYC complex, and $PTCC$ the PER-TIM-CLK-CYC complex.

quantity CC_n represents CLK-CYC that is not in a complex with either PER or TIM. Since PER-CYC-CLK is assumed to have no transcriptional activity, it is not included in these expressions.

(5) PER is intrinsically a nuclear protein, while TIM is intrinsically cytoplasmic. That is, in the absence of posttranslational modfications (via kinase activity or association with other proteins), PER tends to accumulate in the nucleus while TIM tends to accumulate in the cytoplasm (see Figure 1 for the pathways of PER and TIM into the nucleus). The model does not account for the possibility that nuclear TIM may translocate back to the cytoplasm since Meyer and Young (2006) did not see significant evidence of such behavior. PER has a direct pathway to the nucleus (via the term $u_{PER}PER_c$), and so, in the absence of SGG and DBT, PER can enter the nucleus and suppress CLK-activated transcription.

(6) We assume that PER is always in a complex with DBT, and that the initial effect of DBT on PER is to greatly increase its rate of degradation. PER_c is the abundance of PER protein in the cytoplasm that is not in a complex with TIM and for which the effect of DBT is to promote degradation. Hence we expect PER_c to have a very high rate of degradation d_{PER}. (To model the absence of functional DBT, we set $d_{PER} = d_N$, the generic value.) Note that the d_{PER} term represents DBT-mediated degradation of PER, not phosphorylation. After multiple phosphorylations and possibly other modifications, the action of DBT on PER changes (we call this "fully modified" PER and label it PER_c^*), allowing PER to enter the nucleus and remain stable there.

(7) SGG phosphorylates TIM in the cytoplasm (TIM_c), including TIM associated with PER (PT_c), resulting in the modified form PT_c^*. After sufficient modification, TIM dissociates from PER, becoming TIM_c^*, and

then translocates to the nucleus to become TIM_n. TIM cannot translocate to the nucleus without first being modified while dimerized with PER.

(8) Light degrades only TIM protein. The effect of light on the PER-TIM complex is to release PER by degrading TIM, in accordance with the findings of Zeng et al. (1996). To model this effect of light, terms with rate constant d_L are subtracted from quantities involving TIM, and added to those quantities representing the remainder of the complex. For example, if light degrades TIM that is currently part of PER-TIM-CLK-CYC complexes in the nucleus, then the quantity $PTCC_n$ decreases at a rate of $d_L PTCC_n$ and the quantity PCC_n increases at that same rate (some PER-TIM-CLK-CYC changes to PER-CLK-CYC).

Parameters were chosen using a coordinate search method, similar to that described by Forger and Peskin (2003), using data from Lee et al. (1998), Bae et al. (2000), and Shafer et al. (2002). The data are from small vLNs when available, otherwise from head extracts, as indicated in Figure 3, for flies entrained to a 12:12 LD cycle and then released for a day into constant darkness. The detailed data gathered by Shafer et al. (2002) for cytoplasmic and nuclear PER and TIM levels in the small vLNs are particularly useful for our purpose. Since the units of abundance of RNAs and proteins are arbitrary in the model simulations (and in most experimental results), we reduce the number of parameters by normalizing the variables so that the transcription rates v_{clk}, v_{per}, and v_{tim} effectively equal 1 (through a change of variables, e.g., $Clk_{m(new)} = Clk_m/v_{clk}$), and the PER translation rate v_{PER} also equals 1 (by scaling all protein quantities with respect to v_{PER}). This eliminates redundancy in the parameter space, so that the coordinate search will be more

efficient. The simulations mimic the experimental method of entrainment to an LD cycle followed by a day of constant darkness. Since the intrinsic period is important in this protocol, the period of the model was adjusted by rescaling the rate parameters after each parameter change so that the free-running period is always 23.9h in the coordinate search simulations. All simulations were run in Matlab using ode45 as the main solver. The method described here resulted in the parameter values listed in Table 1.

The parameter values (listed in Table 1) selected by the coordinate search to fit the data have some interesting implications. The value $s = 0.27$ indicates that PER-TIM is indeed only partially effective in suppressing the transcriptional activity of CLK-CYC. The rate of CLK synthesis (v_{CLK}) is several fold lower than that for PER (v_{PER}), consistent with the fact that CLK is a limiting factor in the *Drosophila* molecular clock (Bae et al., 2000). The rate of TIM synthesis v_{TIM} is surprisingly low and the degradation rate d_{TIM} is fairly high, but this is balanced by the stability of TIM when in a complex with PER, so that reasonably high levels do accumulate during the cycle. These values may explain why PER peaks earlier than TIM in the cycle (see Figure 3). The linear degradation rate d_{PER} for partially modified PER (without TIM) in the cytoplasm is extremely high while the Michaelis degradation constant is surprisingly low, so DBT-mediated degradation of PER is a strongly linear process in the model. The rate constant h_{PT} for formation of PER-TIM complex in the cytoplasm is extremely high, so these complexes take very little time to form. In contrast, the Michaelis constant p_{TIM} for phosphorylation (and whatever other posttranslational processes the PER-TIM complex undergoes in the cytoplasm) is modest, so that this process takes several hours. The dephosphorylation rate q_{PT} for PER-TIM is quite low, so dephospho-

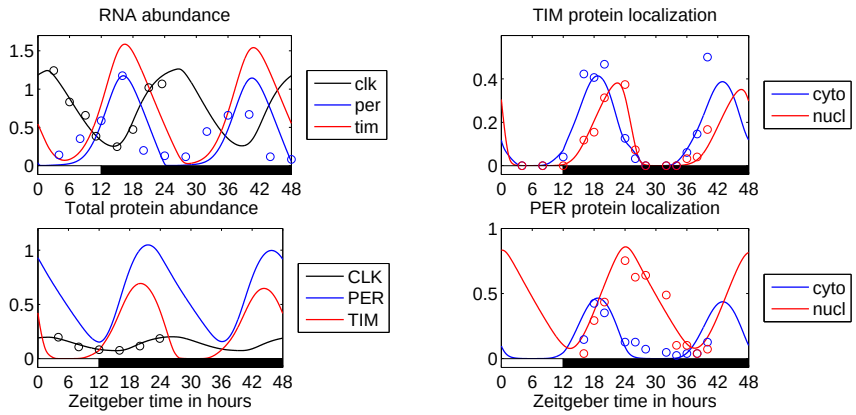

Fig. 3. Simulations of the model given in Figure 2 and the parameter values listed in Table 1. The circles indicate datapoints from experiments used to fit parameters in coordinate search method. The data for *clk* RNA (of head extracts) are from (Lee et al., 1998), while data for total CLK protein and *per* mRNA (of head extracts) are from (Bae et al., 2000). The data for cytoplasmic and nuclear levels of PER and TIM (of small vLNs) are from (Shafer et al., 2002). All data are from Canton S wild type flies.

rylation plays a very minor role in the model. The rate constant h_{PTC} for association of TIM and PER-CLK-CYC is very high, so once TIM enters the nucleus, it rapidly forms a complex with PER-CLK-CYC, thereby partially suppressing transcriptional activation of *per* and *tim*.

The model displays the essential characteristics of a circadian clock. It continues to exhibit robust oscillations when any parameter is varied by up to 20% from the values listed in Table 1, for which the model produces oscillations with free-running period 23.9h. Also see Table 1 for the effect of parameter value changes on the free-running period. The model entrains to LD cycles by means of the TIM degradation parameter d_L, which is set to 0.5 in the presence of light and to 0 in darkness. A photic phase response curve (PRC) for the model is obtained by setting $d_L = 1$ for 2 hours (to simulate the response

to an intense light pulse) during the otherwise constant darkness following entrainment to an LD cycle. See Figure 4A, which was generated via 90 simulations, with a pulse given at a different time in each simulation. The crossover point between advances and delays is early in the simulation, after 5 hours of darkness, rather than after 7 hours as observed in (Stanewsky et al., 1998; Bao et al., 2001). This is an improvement over the PRC of the model of Ueda et al. (2001) for which the crossover point is only 2 hours into darkness. This improvement is likely due to the assumption that PER-TIM only partially inhibits CLK-CYC's transcriptional activities, since changing the partial inhibition to total inhibition ($s = 0$) in the model moves the crossover point in the PRC several hours earlier. The current model remains imperfect in its light response predictions since it does not include CRYPTOCHROME (CRY). TIM degradation is mediated via the response of CRY to light and so the abundance and localization of CRY at the time of the pulse could play an important gating role in phase resetting. For the effect of non-photic pulses on the phase, see Figures 4B and 4C and the discussion at the end of the article.

The relative amounts and peak times of the proteins are accurately predicted by the model. In fly head extracts, CLK is present in limiting amounts, with peak CLK abundance roughly 1/5 that of PER and TIM peak levels; see Figure 4 of (Bae et al., 2000). While our coordinate search routine did not explicitly consider relative peak levels of CLK and PER proteins, the resulting parameters yield a total CLK peak equal to 1/5.3 of the peak PER level (when entrained to a 12:12 LD cycle). Lee et al. (1998) found total TIM peaking before PER in experiments, which is reproduced by our model as shown in Figure 3, but is not predicted by model of Ueda et al. (2001), for which TIM and PER have identical oscillations.

Further support for this model's description of posttranslational behavior of PER and TIM lies in its prediction of the effect of SGG on period length. Martinek et al. (2001) propose that SGG promotes the phosphorylation of TIM in the cytoplasm, and find that overexpression of SGG leads to shortened

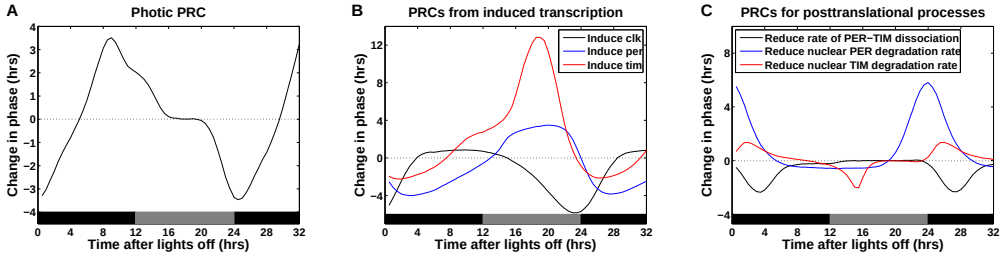

Fig. 4. A. Anchored photic PRC. Light pulses are given (in otherwise constant darkness) following the last lights-off after entrainment to a 12:12 LD cycle (12 hours with $d_L = 0.5$ followed by 12 hours with $d_L = 0$). To simulate response to a short intense light pulse, we set $d_L = 1$ for 2 hours beginning at the indicated time after lights off (otherwise $d_L = 0$). A phase advance is plotted as a positive change in phase, while a phase delay is plotted as a negative change in phase. The phase shift is calculated by comparing the peak of oscillations after 7 days to an unpulsed "control" simulation, to mimic the experimental procedure of comparing behavior of pulsed flies with that of control flies, e.g., as done by Bao et al. (2001). The black bars mark subjective night and the gray bar marks subjective day. B. Induced transcription PRC. A clock gene is induced for 2 hours by adding a constant rate of transcription (1 for *clk* and *per*, 0.2 for *tim*) following the last lights-off after entrainment to a 12:12 LD cycle. C. PRC generated by manipulating posttranslational processes. The black curve shows the PRC generated by reducing the rate m_{PT} of disassociation of modified PER-TIM in the cytoplasm (PT_c^*) to one-fifth its normal value for 2 hours. The blue curve shows the PRC generated by reducing the degradation rate d_{13} of PER in the nucleus (PER_n) to one-fifth its normal value for 2 hours. The blue curve shows the PRC generated by reducing the degradation rate d_{14} of TIM in the nucleus (TIM_n) to one-fifth its normal value for 2 hours.

periods and underexpression to lengthened periods. Our model's predictions agree with this effect of SGG on the period. For example, decreasing p_{TIM} by 10% leads to a lengthened period of 25.1h, while increasing by 10% leads to a shortened period of 23.0h (see Table 1).

Setting v_{TIM} to 0 (so no functional TIM protein is produced, as in a tim^0 mutant) leads to loss of oscillations with a very low constitutive PER level of 0.18, compared to the peak value of 1.05 for PER in the full model. This agrees well with the finding of Price et al. (1995) that loss of functional TIM leads to very low constitutive PER levels of roughly 10% of the wild type peak value. If v_{PER} is set to 0 (so no functional PER protein is produced, as in a per^0 mutant), then the model predicts that TIM will accumulate in the cytoplasm (with a constitutive level of 5.44 in the cytoplasm only, compared to a normal peak value of 0.66 for total TIM), which agrees with the observations of Myers et al. (1996).

Decreasing d_{PER} (to increase stability of PER_c) shortens the predicted period (speeds up the cycle), while increasing d_{PER} (to decrease stability of PER_c) lengthens it (see Table 1). Simulating the absence of functional DBT by setting d_{PER} equal to d_N results in a very short period (17h) rhythm with high levels of PER and very low levels of TIM (see Figure 5). Price et al. (1998) observed apparently constitutive PER and almost no TIM for larval dbt^p mutants in constant darkness, but this could be difficult to distinguish from a small amplitude and short period oscillation, given that samples were taken only 2-3 times per day. Whether oscillations occur may also depend on which type of lateral neuron is sampled. It is particularly interesting to note that the model predicts that *tim* expression will be greatly reduced in the absence of DBT, without any assumption of a direct effect of DBT on *tim* products.

To more appropriately model lack of functional DBT, further details should be added to the model.

Oscillations with constant transcription of one or two clock genes. Antiphase oscillation of *clk* with *per* and *tim* appears to be unnecessary in generating robust oscillations. This is in accord with experimental results of Kim et al. (2002), who found that circadian regulation was largely unaffected in transgenic flies where *per* regulatory sequences were used to drive rhythmic transcription of *clk*. The total level of CLK protein in the nucleus can be held constant, as in Figure 6, with oscillations depending on the association of CLK-CYC with PER or PER-TIM in the nucleus, rather than any change in the total abundance of CLK-CYC. Robust oscillations can also be generated if the transcription rate of *clk* is held constant; see Figure 7.

Robust oscillations can be achieved with constant levels of RNA in two clock genes. With a constant *clk* transcription rate of 1.0 and a constant *per* transcription rate between 0.25 and 0.9 (see Figure 8 for an example using a constant *per* transcription rate of 0.3), the model shows robust oscillations with free-running periods in the range 18-60h (where increasing the rate de-

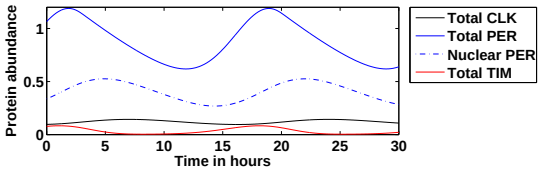

Fig. 5. Simulation showing protein levels in the absence of functional DBT, modeled by setting d_{PER} equal to d_N (so d_{PER}=0.02), that is, we assume the main effect of DBT is to increase the degradation rate of cytoplasmic PER. The model predicts a very short period rhythm (17h) with high levels of PER and very low levels of TIM (without any assumption of a direct effect of DBT on *tim*).

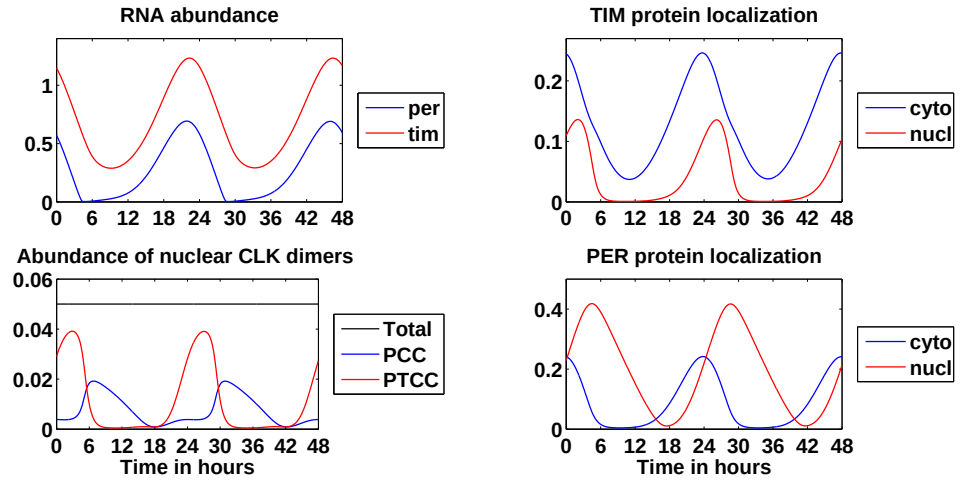

Fig. 6. Example of free-running oscillations with a constant level of CLK-CYC (entirely in nucleus). The first three equations of the full model in Figure 2 are neglected, as is any degradation of CLK protein. Total abundance of CLK is fixed at 0.05. Remaining parameters are as listed in Table 1.

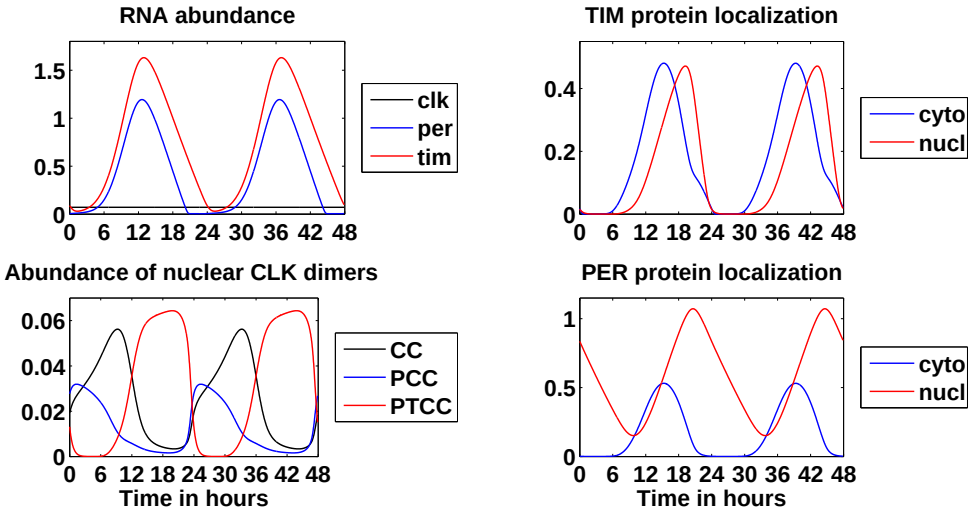

Fig. 7. Example of free-running oscillations with a constant rate of transcription of *clk* (resulting in a constant level of *clk* RNA). The constant rate of *clk* transcription is achieved by replacing the term $\frac{v_{clk}k_1^2}{k_1^2+(CC_n+sPTCC_n)^2}$ with the value v_{clk} in the first equation of the model given in Figure 2. All parameters are as listed in Table 1. The free-running period is 26.9h.

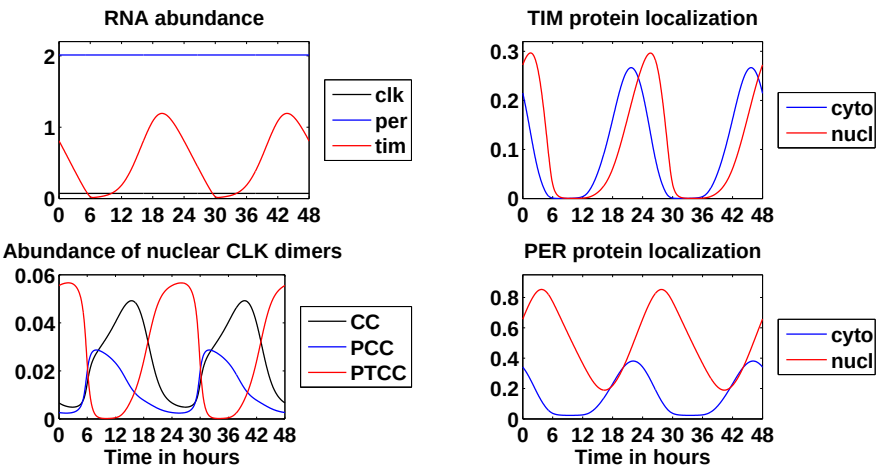

Fig. 8. Robust oscillations with a constant rate of transcription of *clk* and *per*. The constant rate of *clk* transcription is as described in Figure 7, while a constant rate of *per* transcription is achieved by replacing the term $\frac{v_{per}(CC_n+sPTCC_n)^2}{k_5^2+(CC_n+sPTCC_n)^2}$ with $.3v_{per}$. All parameter values are as listed in Table 1. The free-running period is 23.6h.

creases the period, with very low amplitude rhythms at the extreme ends of the range). Other values for the constant rate of transcription yield steady state (arrhythmic) solutions. The model can also produce oscillations with a constant rates of *clk* and *tim* transcription, which tend to have strong PER oscillation but weaker TIM oscillation. For example, a constant *clk* transcription rate of 0.2 yields oscillations for a constant *tim* transcription rate between 0.3 and 0.6, with periods in the narrow range 23.5-25.2h, with period increasing as the transcription rate increases (see Figure 9 for an example using a constant rate of 0.4). Higher constant transcription rates of either *clk* or *tim* result in very large accumulations of TIM in the cytoplasm. Note that in Figure 9 that while TIM levels in the cytoplasm are high with a small amplitude oscillation, TIM levels in the nucleus exhibit a strong rhythm, so it is possible for rhythms to persist despite large, nearly constitutive levels of total TIM accumulation.

Simulation of a per^{01}-tim^{01} double rescue.

While it is not possible to produce oscillations in this model with constant transcription of both *per* and *tim*, the model does suggest a possible mechanism for the rescue of per^{01}-tim^{01} mutants in the experiments of Yang and Sehgal (2001). We conjecture that the TIM^{01} protein is partially functional, based on the 5% of tim^{01} flies with rhythmicity, as observed by Sehgal et al. (1994). We can model reduced functionality of TIM protein via reduced quantities, for example, by significantly decreasing the *tim* maximum transcription rate v_{tim}. If $v_{tim} < .45$, arrhythmia occurs. Hence the TIM^{01} protein can be partially functional and yet no rhythms are generated. See Figure 10. Those few tim^{01} flies that show some rhythmicity may have TIM^{01} with just barely sufficient functionality to generate weak rhythms.

Based on this idea, we model a per^{01}-tim^{01}-type mutant by setting the *per* maximum transcription rate v_{per} equal to 0 (no functional PER produced) and reducing the *tim* maximum transcription rate v_{tim} to 28% of its normal

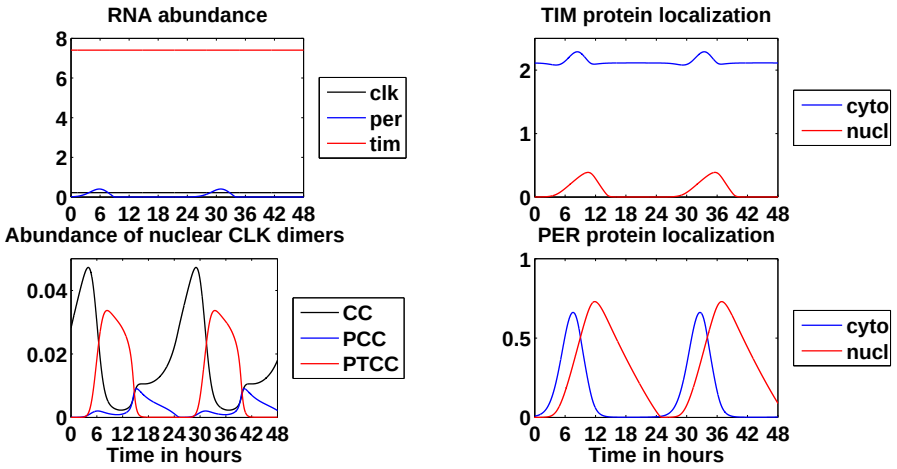

Fig. 9. Robust oscillations with a constant rate of transcription of *clk* and *tim*. The constant rate of *clk* transcription is $0.2v_{clk}$, and the constant rate of *tim* transcription is achieved by replacing the term $\frac{v_{tim}(CC_n+sPTCC_n)^2)}{k_6^2+(CC_n+sPTCC_n)^2}$ with $0.4v_{tim}$. All parameter values are as listed in Table 1. Free-running period in this simulation is 25.1h.

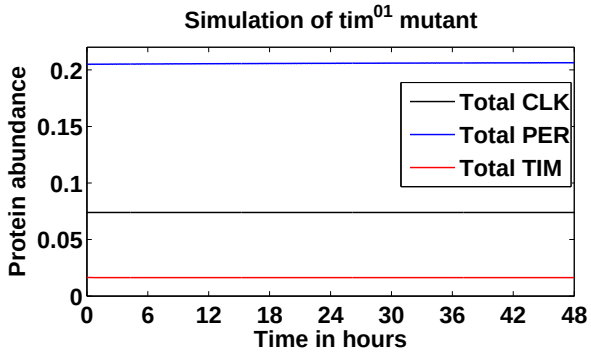

Fig. 10. Simulation of an arrhythmic tim^{01}-type mutant. The *tim* maximum transcription rate v_{tim} is reduced to 40% of its normal value, in order to model reduced functionality of TIM protein via reduced quantities.

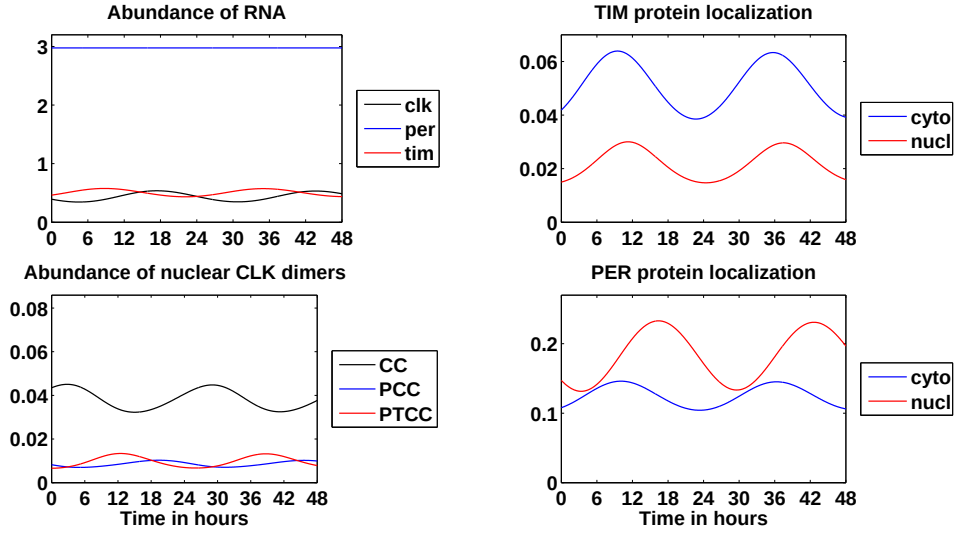

Fig. 11. Simulation of the double-rescue of a per^{01}-tim^{01}-type mutant. The *per* maximum transcription rate v_{per} is set equal to 0 (no functional PER produced) and the *tim* maximum transcription rate v_{tim} is reduced to 28% of its normal value (as listed in Table 1), in order to model reduced functionality of TIM protein via reduced quantities. Constant transcription rates 0.32 for *per* and 0.16 for *tim* are added to the right hand sides of the equations for $\frac{dPer_m}{dt}$ and $\frac{dTim_m}{dt}$ in Figure 2 to mimic the rescue experiments of Yang and Sehgal (2001). This restores rhythmicity to the nuclear protein levels, with free-running period 26.2h in DD.

value (as listed in Table 1), which results in arrhythmia. The rescue of this per^{01}-tim^{01}-type mutant can be achieved by adding constant transcription rates 0.32 for *per* and 0.16 for *tim* to the right hand sides of the equations for $\frac{dPer_m}{dt}$ and $\frac{dTim_m}{dt}$ in Figure 2, to mimic the rescue experiments of Yang and Sehgal (2001). This results in a free-running rhythm with period 26.2h, similar to the mean period of 26.9h given by Yang and Sehgal (2001) for a particular per^{01}-tim^{01} rescue experiment in which 52% of flies were rhythmic. See Figure 11 for a simulation. In general, the rescue experiments of Yang and Sehgal (2001) show great variability in period, both shorter and longer than 24h, and in our model a similarly wide range of free-running periods can be generated by altering the parameter values for the constant transcriptions rates of *per* and *tim*. Note that the oscillation of *tim* mRNA in Figure 11 is of very low amplitude and would likely appear constitutive in experiments, consistent with the finding of constitutive *tim* mRNA in the double rescue experiments of Yang and Sehgal (2001). In addition, *clk* expression is significantly down-regulated in the simulations shown in Figures 10 and 11, although the parameters regulating *clk* expression are unchanged from "wild-type" (Table 1). This is also in agreement with the experimental findings of Yang and Sehgal (2001).

Simulation of per^S, per^L, and tim^{UL} mutants.

We can also use the model to simulate three additional clock gene mutations: per^S, per^L, and tim^{UL}. Marrus et al. (1996) found that the per^S mutation leads to a truncated nuclear protein accumulation phase and so to a premature RNA increase, resulting in a very short period of 19h. Meyer and Young (2006) observed that the per^L mutation delayed nuclear accumulation in vivo without affecting rates of PER-TIM assembly, resulting in a period of 28h and

mean onset of nuclear accumulation 152 min later (on average) than for *per*. They hypothesize that the per^L mutation likely reduces the rate of PER-TIM dissociation. Meyer and Young (2006) also observed that the tim^{UL} mutation delays PER and TIM nuclear turnover, leading to a 33h period, with no effect on timing of nuclear translocation. To model these mutations, we use parameter values as listed in Table 1, except for the following: PER_n degradation constants are increased to $d_{13} = 0.064$ and $g_{13} = 0.08$ to mimic the truncated

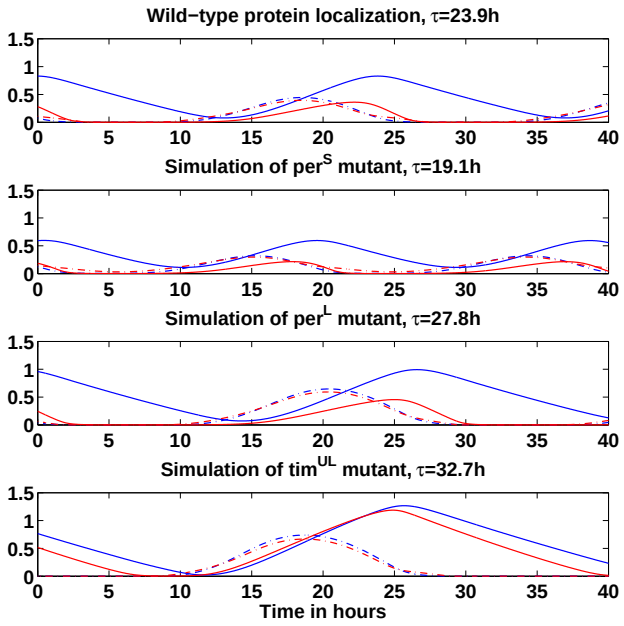

Fig. 12. Simulations mimicking three clock gene mutations: per^S, per^L, and tim^{UL} (free-running in DD). The dashed blue curve gives total cytoplasmic PER levels and the solid blue curve gives total nuclear PER levels, while the dashed red curve gives total cytoplasmic TIM levels and the solid red curve gives total nuclear TIM levels. The parameters are as listed in Table 1, except for the following: the PER_n degradation constants are increased to $d_{13} = 0.064$ and $g_{13} = 0.08$ to mimic per^S; the rate m_{PT} of PER-TIM dissociation in the cytoplasm is reduced to one-third of its normal value to mimic per^L; and the nuclear TIM degradation rate d_{14} is reduced to 0.066 to mimic tim^{UL}.

nuclear protein accumulation phase of per^S; the rate m_{PT} of PER-TIM dissociation in the cytoplasm is reduced to one-third of its normal value to mimic the delayed nuclear translocation rate of the PER^L protein via a reduced rate of PER-TIM dissociation in the cytoplasm; and the nuclear TIM degradation rate d_{14} is reduced to 0.066 to mimic the reduced degradation rate of nuclear TIM^{UL}. These altered parameter values where selected to yield free-running periods 19.1h for per^S, 27.8h for per^L, and 32.7h for tim^{UL}. The protein localization patterns in these simulations are similar to the observed effects of these mutations (Marrus et al., 1996; Meyer and Young, 2006). See Figure 12. Also, despite the very short period in the per^S mutant, the model predicts that it can entrain to a 12:12 LD cycle, which has been observed experimentally by Marrus et al. (1996).

3 Discussion

While we do not deny the importance of rhythmic transcription in the *Drosophila* clock, we feel that the importance of some posttranslational processes has been underestimated. The model presented here begins to address the roles of some of these processes in the clock, but many other processes remain to be addressed, such as posttranscriptional processes, the effects of successive phosphorylation of proteins such as PER and CLK, and the role of phosphatases in the clock mechanism. As experiments continue to reveal more details of the clock, mathematical models can support the development of a more accurate description of the clock mechanism by testing hypotheses. An excellent example is the recent paper by Gallego et al. (2006) that clarified the role of kinase activity in the hamster *tau* mutation.

Our model requires many assumptions and some guesses based on recent experimental results. For example, we hypothesize that DBT's effect on PER depends on the number of phosphorylations. Initially, DBT appears to promote degradation of PER and cause its retention in the cytoplasm. However, PER does eventually move into the nucleus where it appears to be quite stable, although still associated with DBT (but not TIM for some time). Nuclear PER protein persists through the morning following the rapid degradation of TIM (Weber and Kay, 2003). Hence light-induced degradation of TIM speeds up nuclear translocation of PER during early night when PER and TIM are primarily in the cytoplasm, and it increases transcriptional suppression during late night and early morning when PER and TIM are primarily in the nucleus. This suggests that after further phosphorylation of PER, DBT ceases to block the nuclear translocation of PER and also no longer promotes the degradation of PER. This process could parallel that of the mammalian casein kinase Iϵ (a homolog of DBT) that controls the nuclear entry of mammalian PERIOD1 protein (Vielhaber et al., 2000).

PER-TIM dissociation plays important roles.

PER appears to be released from the PER-TIM complex at two different times in the circadian cycle: before nuclear entry in the middle of the night and again around dawn. These dissociations may play important roles in the phase-shifting mechanism of the clock. The *Drosophila* clock does not shift in response to light during subjective day (CT0-10) because TIM is not present. During this time, PER finishes the cycle by fully suppressing the transcriptional activity of CLK-CYC. The *Drosophila* clock delays in response to light pulses during CT10-19, when TIM is mostly present in the cytoplasm. However, it may be important for suppression of CLK-CYC transcriptional activity

to begin before CT19 in order for the cycle to have a 24 hour period. The dissociation of PER and TIM followed by delayed nuclear entry of TIM allows PER to begin suppressing CLK-CYC in the nucleus during CT16-19, during which time the clock continues responding to light by delaying. TIM is strongly present in the nucleus during CT19-24, effectively reducing the suppression of CLK-CYC. If a light pulse occurs during this time, PER is released and so advances the cycle by fully suppressing CLK-CYC.

It is not necessary for PER to enter the nucleus before TIM. Some simulations show PER and TIM entering the nucleus at about the same time, or TIM entering before PER, which typically lengthens the period (e.g., see Figure 11). The experiments of Meyer and Young (2006) also show variability in the relative timing of nuclear entry of PER and TIM. The dissociation of PER and TIM offers the circadian molecular mechanism another means of adjusting the period and phase of the oscillations, through flexibility in the relative timing of the nuclear entry of PER and TIM.

CLK oscillation is unnecessary.

The model exhibits robust oscillations with constitutive CLK, so long as total CLK levels remain well below total PER levels (specifically, if total CLK abundance is between 0.02 and 0.09, yielding free-running periods of 14-35 hours). In fact, Kim et al. (2002) found that the *Drosophila* clock is very modestly altered by *clk* RNA being in phase with *per* and *tim* (rather than the usual antiphase relation), and so rhythmicity of *clk* expression appears to have little functional significance (although perhaps some effect on light response patterns). With CLK levels well below those of PER, it is the timing of PER translocating to the nucleus and so inhibiting CLK's transcriptional activation that is key to the clock oscillation, while the timing of the trough

or peak of overall CLK abundance has little effect.

Minimal rhythmic transcription is sufficient.

As seen in Figures 7-9, oscillations can be achieved with constant levels of RNA of *clk* and *per* or *tim* for a restricted range of values of the transcription rate parameters; outside this narrow range, the model predicts arrhythmia. For a certain range of parameter values, oscillations can also persist with a constant transcription rate of *per* and a reduced rhythmic transcription rate of *tim* enhanced by an additional constant rate. This could explain the appearance of rhythmic individuals in a majority arrhythmic population of mutants with constant transcription rates (Frisch et al., 1994; Vosshall and Young, 1995; Cheng and Hardin, 1998; Yang and Sehgal, 2001). For a small range of rate values, oscillations of a circadian-like period will occur, but outside that range (corresponding to either under- or overexpression of a clock gene), the model predicts that the clock is arrhythmic.

The double rescue simulation in Figure 11 is particularly interesting, as it shows that robust oscillations can persist with constant transcription of *per* and slight oscillations of *clk* and *tim*. While complete loss of oscillations in the transcription of *per* and *tim* always leads to arrhythmia in the model, it is possible to generate oscillations with minimal rhythmic transcription, due to various posttranslational mechanisms amplifying the weak transcriptional rhythm. Particularly important mechanisms appear to be the delay resulting from the TIM sequestering PER in the cytoplasm until the dissociation of the PER-TIM complex, the differential times of nuclear entry of PER and TIM, and the partial suppression of PER-TIM versus the total suppression of PER on the transcriptional activity of CLK-CYC. Some of these mechanisms are strongly associated with kinase activity, with DBT and SGG playing key roles.

Suggested experiments to validate model.

We have tested our model's predictions against many known experimental results. For the most part, the model reasonably reproduces these results. One possible exception is its prediction of rhythmicity (with very short period) in the absence of functional DBT. It would be interesting to see the experiments of Price et al. (1998) done with more frequent time sampling (of the small vLNs, if possible) in order to compare to our simulation (which itself has some weaknesses in not fully accounting for all of the possible effects of DBT in cytoplasm and nucleus). Our model does reproduce their finding that TIM levels are suppressed, so some features do match the experimental data.

We have also generated some simulations that do not correspond to experiments in the literature (to our knowledge). We simulated the effects on nuclear localization of PER and TIM of the per^L and tim^{UL} mutations, to compare to the experiments of Meyer and Young (2006). We also simulated the effects of the per^S mutation, and it would be interesting to see how that compares to an experiment with per^S like those of Meyer and Young (2006).

Another set of simulations that would be interesting to compare to experiments in order to test the model are shown in Figures 4B and 4C: PRCs that result from pulses (at different times of day) of induced clock gene expression or of suppression of certain posttranslational mechanisms. We generated these PRCs in order to explore when the system is most sensitive to these processes and how changes to them affect the phase of the clock. The clock gene induction PRC could perhaps be generated experimentally through heat pulses, with gene expression induced by a heat shock promoter. The model predicts that inducing *clk* during the last part of subjective day or during early subjective night delays the clock , but has little effect on the clock the rest of

the time. In contrast, inducing *per* causes delays during subjective night and advances during subjective day. The clock is very sensitive to *tim* induction; a modest pulse of induced transcription (only a fifth the value of the rates used for *clk* or *per*) causes very large advances during subjective day, and smaller delays during subjective night. Under constant conditions, the TIM level during subjective day is essentially zero, so inducing *tim* transcription during the subjective day (in DD) starts the next cycle and so advances the phase. See Figure 4B.

Figure 4C shows effect of decreasing the rate of important posttranslational processes at different times of day. Reducing the rate of PER-TIM dissociation causes modest delays during the first half of subjective night (the part of the cycle when PER-TIM is at high levels in the cytoplasm and nuclear entry of PER and TIM would normally begin), but little effect otherwise. Reducing the degradation rate of nuclear PER protein results in large advances around subjective dusk (when nuclear PER levels are peaking; retaining PER longer prolongs the suppression of CLK-CYC and so more quickly finishes the current cycle). Reducing the degradation rate of nuclear TIM protein during the first half of subjective day causes small delays (TIM levels at this times are normally decreasing, so slowing the degradation delays the vanishing of TIM), and during the first half of subjective night causes small advances (when TIM levels are increasing, so decreasing the degradation rate speeds up the accumulation of TIM).

The model also predicts that a "triple rescue" experiment may be possible. If *clk* and *per* transcription rates are constant, while *tim* transcription is nearly constant (in the sense of the double rescue simulation in Figure 11), then the posttranslational mechanisms sufficiently amplify this slight rhythm into

a robust rhythm in the nuclear proteins. See Figure 13. The relatively large constant transcription rate for *per* leads to cytoplasmic accumulation of PER. The free running period is prolonged due to gradual increase of TIM in the cytoplasm, eventually followed by PER nuclear entry.

In conclusion, our model is detailed enough that it captures many of the important features of observed clock gene expression and the consequences of various mutations and other changes of the molecular clock, including those involving the localization of PER and TIM. In particular, the modeling in this paper supports the idea that posttranslational processes play key roles in generating as well as modulating robust circadian oscillations. It appears

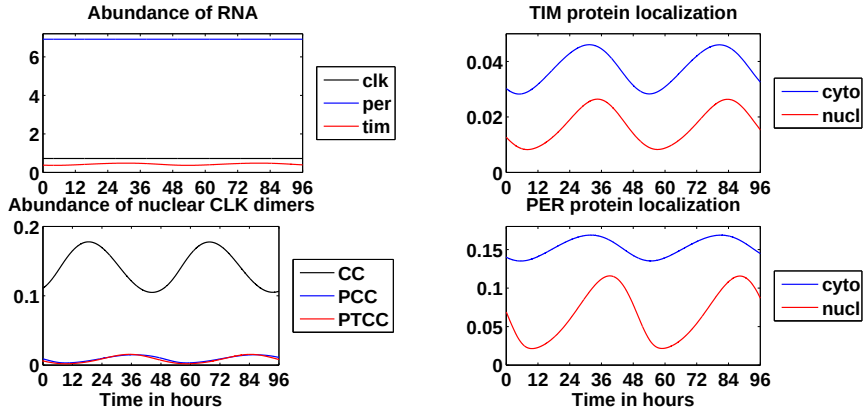

Fig. 13. Simulation of the triple rescue of a clk^0-per^{01}-tim^{01}-type mutant. The *clk* and *per* maximum transcription rates v_{clk} and v_{per} are set equal to 0 (to simulate no functional CLK or PER proteins being produced), while the *tim* maximum transcription rate v_{tim} is reduced to 12% of its normal value (as listed in Table 1), in order to model reduced functionality of TIM protein via reduced quantities. This leads to arrhythmicity in the model. To "rescue" the rhythm, constant transcription rates 0.5 for *clk*, 0.4 for *per*, and 0.15 for *tim* are added to the right hand sides of the equations for $\frac{dClk_m}{dt}$, $\frac{dPer_m}{dt}$, and $\frac{dTim_m}{dt}$ in Figure 2. This restores rhythmicity of the nuclear proteins, with free-running period 49h in DD. (All other parameters are as listed in Table 1.)

that posttranslational mechanisms alone are not sufficient to generate rhythms in *Drosophila*, but low-amplitude transcriptional rhythms can be amplified by posttranslational mechanisms to yield robust oscillations of the nuclear protein levels.

References

Allada, R., Emery, P., Takahashi, J. S., Rosbash, M., 2001. Stopping time: the genetics of fly and mouse circadian clocks. Annu. Rev. Neurosci. 22, 1091–1119.

Bae, K., Choogon, L., Hardin, P. E., Edery, I., 2000. dCLOCK is present in limiting amounts and likely mediates daily interactions between the dCLOCK-CYC transcription factor and the PER-TIM complex. J. Neurosci. 20, 1746–1753.

Bao, S., Rihel, J., Bjes, E., Fan, J.-Y., Price, J. L., 2001. The *Drosophila double-time*^{S} mutation delays the nuclear accumulation of *period* protein and affects the feedback regulation of *period* mRNA. J. Neurosci. 21, 7117–7125.

Chang, D. C., Reppert, S. M., 2003. A novel C-terminal domain of *Drosophila* PERIOD inhibits dCLOCK:CYCLE-mediated transcription. Curr. Biol. 13, 758–762.

Cheng, Y., Hardin, P. E., 1998. *Drosophila* photoreceptors contain an autonomous circadian oscillator that can function without *period* mRNA cycling. J. Neurosci. 18, 741–750.

Cyran, S. A., Buchsbaum, A. M., Reddy, K. L., Lin, M.-C., Glossop, N. R. J., Hardin, P. E., Young, M. W., Storti, R. V., Blau, J., 2003. *vrille*, *Pdp1*, and *dClock* form a second feedback loop in the *Drosophila* circadian clock. Cell

112, 329–341.

Cyran, S. A., Yiannoulos, G., Buchsbaum, A. M., Saez, L., Young, M. W., Blau, J., 2005. The double-time protein kinase regulates the subcellular localization of the *Drosophila* clock protein period. J. Neurosci. 25, 5430–5437.

Forger, D., Peskin, C., 2003. A detailed predictive model of the mammalian circadian clock. PNAS 100, 14806–11.

Frisch, B., Hardin, P. E., Hamblen, C. M., Rosbash, M., Hall, J. C., 1994. A promoterless *period* gene mediates behavioral rhythmicity and cyclical *per* expression in a restricted subset of the *Drosophila* nervous system. Neuron 12, 555–570.

Gallego, M., Eide, E. J., Woolf, M. F., Virshup, D. M., Forger, D. B., 2006. An opposite role for *tau* in circadian rhythms revealed by mathematical modeling. PNAS 103, 10618–10623, doi/10.1073/pnas.0604511103.

Harms, E., Kivime, S., Young, M. W., Saez, L., 2004. Posttranscriptional and posttranslational regulation of clock genes. J. Biol. Rhythms 19, 361–373, DOI: 10.1177/0748730404268111.

Houl, J. H., Yu, W., Dudek, S. M., Hardin, P. E., 2006. *Drosophila* CLOCK is constitutively expressed in circadian oscillator and non-oscillator cells. J. Biol. Rhythms 21, 93–103, DOI: 10.1177/0748730405283697.

Kim, E. Y., Bae, K., Ng, F. S., Glossop, N. R., Hardin, P. E., Edery, I., 2002. *Drosophila* CLOCK protein is under posttranscriptional control and influences light-induced activity. Neuron 34, 69–81.

Kiyohara, Y. B., Tagao, S., Tamanini, F., Morita, A., Sugisawa, Y., Yasuda, M., Yamanaka, I., Ueda, H. R., van der Horst, G. T. J., Kondo, T., Yagita, K., 2006. The BMAL1 C terminus regulates the circadian transcription feedback loop. PNAS 103, 10074–10079, doi 10.1073/pnas.0601416103.

Kloss, B., Rothenfluh, A., Young, M. W., Saez, L., 2001. Phosphorylation of PERIOD is influenced by cycling physical associations of DOUBLE-TIME, PERIOD, and TIMELESS in the *Drosophila* clock. Neuron 30, 699–706.

Lakin-Thomas, P. L., 2006. Transcriptional feedback oscillators: Maybe, maybe not... J. Biol. Rhythms 21, 83–92, doi 10.1177/0748730405286102.

Lee, C., Bae, K., Edery, I., 1998. The *Drosophila* CLOCK protein undergoes daily rhythms in abundance, phosphorylation, and interactions with the PER-TIM complex. Neuron 21, 857–867.

Lee, C., Etchegaray, J., Cagampang, F., Loudon, A., Reppert, S., 2001. Post-translational mechanisms regulate the mammalian circadian clock. Cell 107, 855–867.

Leloup, J., Goldbeter, A., 2004. Modeling the mammalian circadian clock: Sensitivity analysis and multiplicity of oscillatory mechanisms. J. Theor. Biol. 230, 541–562.

Leloup, J. C., Goldbeter, A., 1998. A model for circadian rhythms in *Drosophila* incorporating the formation of a complex between the PER and TIM proteins. J. Biol. Rhythms 13, 70–87.

Levine, J. D., 2004. Sharing time on the fly. Curr. Opin. Cell Biol. 16, 210–216.

Marrus, S. B., Zeng, H., Rosbash, M., 1996. Effect of constant light and circadian entrainment of per^s flies: evidence for light-mediated delay of the negative feedback loop in *Drosophila*. EMBO J. 15 (24), 6877–6886.

Martinek, S., Inonog, S., Manoukian, A. S., Young, M. W., 2001. A role for the segment polarity gene *shaggy*/GSK-3 in the *Drosophila* circadian clock. Cell 105, 769–779.

Meyer, P., Young, M., 2006. PER-TIM interactions in living *Drosophila* cells: An interval timer for the circadian clock. Science 311, 226–229.

Myers, M. P., Wager-Smith, K., Rothenfluh-Hilfiker, A., Young, M., 1996.

Light-induced degradation of TIMELESS and entrainment of the *Drosophila* circadian clock. Science 271, 1736–1740.

Nakajima, M., Imai, K., Ito, H., Nishiwaki, T., Murayama, Y., Iwasaki, H., Oyarna, T., Kondo, T., 2005. Reconstitution of circadian oscillation of cyanobacterial KaiC phosphorylation in vitro. Science 308, 414–415.

Price, J. L., 2004. *Drosophila melanogaster*: a model system for molecular chronobiology. In: Sehgal, A. (Ed.), Molecular biology of circadian rhythms. Wiley, Hoboken, NJ, pp. 33–74.

Price, J. L., Blau, J., Rothenfluh, A., Abodeely, M., Kloss, B., Young, M. W., 1998. *double-time* is a novel *Drosophila* clock gene that regulates PERIOD protein accumulation. Cell 94, 83–95.

Price, J. L., Dembinska, M. E., Young, M. W., Rosbash, M., 1995. Suppression of PERIOD protein abundance and circadian cycling by the *Drosophila* clock mutation *timeless*. EMBO J. 14, 4044–4049.

Rieger, D., Shafer, O. T., Tomioka, K., Helfrich-Förster, C., 2006. Functional analysis of circadian pacemaker neurons in *Drosophila melanogaster*. J. Neurosci. 26 (9), 2531–2543.

Rothenfluh, A., Young, M. W., Saez, L., 2000. A TIMELESS-independent function for PERIOD proteins in the *Drosophila* clock. Neuron 26, 505–514.

Ruoff, P., Christensen, M. K., Sharma, V. K., 2005. PER/TIM-mediated amplification, gene dosage effects and temperature compensation in an interlocking-feedback loop model of the *Drosophila* circadian clock. J. Theor. Biol. 237, 41–57, doi:10.1016/j.jtbi.2005.03.030.

Sehgal, A., Price, J. L., Man, B., Young, M. W., 1994. Loss of circadian behavioral rhythms and *per* RNA oscillations in the *Drosophila* mutant *timeless*. Science 263, 1603–1606.

Shafer, O. T., Rosbash, M., Truman, J. W., 2002. Sequential nuclear accu-

mulation of the clock proteins PERIOD and TIMELESS in the pacemaker neurons of *Drosophila melanogaster*. J. Neurosci. 22, 5946–5954.

Smolen, P., Hardin, P. E., Lo, B. S., Baxter, D. A., Byrne, J. H., 2004. Simulation of *Drosophila* circadian oscillations, mutations, and light responses by a model with VRI, PDP-1, and CLK. Biophys. J. 86, 2786–2802.

Stanewsky, R., Kaneko, M., Emery, P., Beretta, B., Wager-Smith, K., Kay, S. A., Rosbash, M., Hall, J. C., 1998. The *cry^b* mutation identifies cryptochrome as a circadian photoreceptor in *Drosophila*. Cell 95, 681–692.

Ueda, H. R., Hagiwara, M., Kitano, H., 2001. Robust oscillations within the interlocked feedback model of *Drosophila* circadian rhythm. J. Theor. Biol. 210, 401–406, doi:10.1006/jtbi.2000.2226.

Vielhaber, E., Eide, E., Rivers, A., Gao, Z., Virshup, D., 2000. Nuclear entry of the circadian regulator *mPer1* is controlled by mammalian casein kinase 1ε. Mol. Cell. Biol. 20, 4888–99.

Vosshall, L. B., Young, M. W., 1995. Circadian rhythms in *Drosophila* can be driven by *period* expression in a restricted group of central brain cells. Neuron 15, 345–360.

Weber, F., Kay, S. A., 2003. A PERIOD inhibitor buffer introduces a delay mechanism for CLK/CYC-activated transcription. FEBS Lett. 555, 341–345, doi: 10.1016/S0014–5793(03)01269–9.

Yang, Z., Sehgal, A., 2001. Role of molecular oscillations in generating behavioral rhythms in *Drosophila*. Neuron 29, 453–467.

Young, M. W., Kay, S. A., 2001. Time zones: a comparative genetics of circadian clocks. Nat. Rev. Genet. 2, 702–714.

Zeng, H., Qian, Z., Myers, M. P., Rosbash, M., 1996. A light-entrainment mechanism for the *Drosophila* circadian clock. Nature 380, 129–135.